**Pharmacogn.** Mag.
A multifaceted peer reviewed journal in the field of Pharmacognosy and Natural Products
www.phcog.com | www.phcog.net

ORIGINAL ARTICLE

# Effects of *Cyclocarya paliurus* Flavonoid Extract in Non-alcoholic Steatohepatitis Mice: Intermeshing Network Pharmacology and *in vivo* Pharmacological Evaluation

**Senling Feng*, Jing Zhang[1,*], Baoying Liang[2], Hongliu Jin, Zhongwen Yuan**

Department of Pharmacy, Key Laboratory for Major Obstetric Diseases of Guangdong Province, The Third Affiliated Hospital of Guangzhou Medical University, 510150, Guangzhou, Guangdong, [1]Department of Pharmacy, Guangzhou Eighth People's Hospital, Guangzhou, Guangdong Province, 510060, [2]Department of Dermatology, The Second Affiliated Hospital of Guangzhou University of Traditional Chinese Medicine, Guangdong Provincial Hospital of Traditional Chinese Medicine, Guangzhou, Guangdong 510120, P.R. China
*These authors have contributed equally to this work

Submitted: 15-Jan-2021 Revised: 05-Aug-2021 Accepted: 09-Sep-2021 Published: 24-Jan-2022

## ABSTRACT

**Objectives:** Non-alcoholic steatohepatitis (NASH) is the second most common cause of the hepatitis. In this study, we aimed to investigate the effects and mechanisms of *Cyclocarya paliurus* (CPF) flavonoids extract in the treatment of NASH. To achieve this, we performed compound target prediction and network analysis based on the method of network pharmacology. We investigated the effect of CPF extract on NASH and the underlying molecular mechanisms using the *in vivo* pharmacological evaluation technique. **Materials and Methods:** First, NASH was induced in mice with a high-fat diet. Furthermore, experimental validation was carried out with a high-fat feed-induced NASH mouse model. Chemical compounds and human target proteins of CPF, as well as NASH-related human genes, were obtained from TCMSP, PubChem, and GenBank Database, respectively. Subsequently, molecular networks and typical pathways presumably involved in the treatment of CPF on NASH were performed by Metoscape and String software. Then, the network was constructed by using Cytoscape v3.7.2. The Kyoto Encyclopedia of Genes and Genomes pathway enrichment was performed by using Database for Annotation. Then, the possible underlying mechanisms were studied using the quantitative reverse transcription polymerase chain reaction and Western blot analysis. **Results:** The network pharmacology research showed that the CPF, which contained 26 compounds and 27 genes, regulated the most signaling pathways related to NASH. Moreover, the protein–protein interaction network based on the targets of CPF on NASH revealed that the core compounds were luteolin, quercetin, kaempferol, ellagic acid, isoquercitrin, gallic acid, inositol, and myricetin, which were regulated by more than 4 compounds, remarkable related with peroxisome proliferator-activated receptor (PPAR) signaling pathway, cholesterol metabolism, bile secretion, type II diabetes mellitus, adenosine 5′-monophosphate-activated protein kinase signaling pathway, and insulin signaling pathway. In addition, carnitine palmitoyltransferase 2, cytochrome P450 family 7 subfamily A member 1 (CYP7A1), cytochrome P450 family 27 subfamily A member 1 (CYP27A1), and fatty acid-binding protein 1 were treated as target genes of CPF in NASH. *In vivo* experiments indicated that CPF promoted Peroxisome proliferator-activated receptor alpha (PPAR α)/ Peroxisome proliferator-activated receptor gamma (PPAR γ) signaling pathway in NASH mouse model. **Conclusion:** CPF played a role in inhibiting lipid response in NASH, which was closely associated with the modulation effect of CPF on PPAR α/PPAR γ signaling pathway.

**Key words:** *Cyclocarya paliurus* flavonoids, non-alcoholic steatohepatitis mice, network pharmacology, non-alcoholic steatohepatitis, peroxisome proliferator-activated receptor α/γ

## SUMMARY

- In this study, we examined the efficacy of *Cyclocarya paliurus* (CPF) on high-fat diet-induced non-alcoholic steatohepatitis (NASH) mice. Compared with the model group, the CPF-treated mice showed less weight gain and reduced the levels of total cholesterol and triglyceride and showed a significant reduction in the levels of alanine aminotransferase, aspartate aminotransferase (AST), and malondialdehyde.
- Then, we investigated the mechanism of action of CPF in the treatment of NASH through target prediction and network analysis. We found that the core genes that were significantly associated with peroxisome proliferator-activated receptor (PPAR) signaling pathway was peroxisome proliferator-activated receptor alpha, peroxisome proliferator-activated receptor gamma, carnitine palmitoyltransferase 2, fatty acid binding protein 1, CYP7A1, and CYP27A1. The evaluation of mRNA levels and proteins was accomplished by the quantitative reverse transcription polymerase chain reaction and Western blot analysis. According to our results, CPF has a potent effect in lowering the levels of fat accumulation in the liver and shows anti-steatogenic effect by the activation of PPAR signaling pathway in C57BL/6J mice. CPF might be used in the prevention and treatment of NASH.

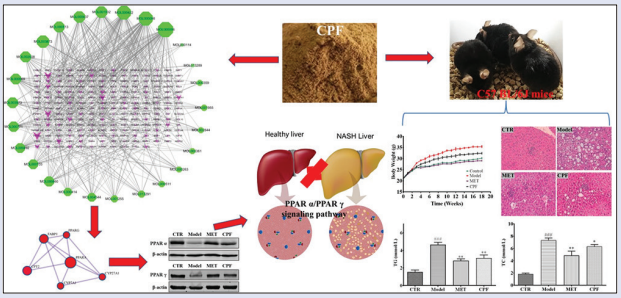


**Abbreviations used:** CPF: *Cyclocarya paliurus*; NASH: Non-alcoholic steatohepatitis; MET: Metformin; TG: Triglyceride; TC: Total cholesterol; ALT: Alanine aminotransferase; AST: Aspartate transaminase; MDA: Malondialdehyde; SOD: Superoxide dismutase; PPAR α: Peroxisome proliferator-activated receptor alpha; PPAR γ: Peroxisome proliferator-activated receptor gamma; CYP7A1: Cholesterol 7-alpha-hydroxylase; CYP27A1: Cholesterol 27-alpha-hydroxylase; FABP1: Fatty acid-binding protein 1; CPT2: Carnitine Palmitoyltransferase 2.

**Correspondence:**

Dr. Zhongwen Yuan,
Department of Pharmacy,Key Laboratory for Major Obstetric Diseases of Guangdong Province, The Third Affiliated Hospital of Guangzhou Medical University, 510150, Guangzhou, Guangdong, P.R. China.
E-mail: 2018681079@gzhmu.edu.cn
**DOI:** 10.4103/pm.pm_21_21

**Access this article online**
**Website:** www.phcog.com
**Quick Response Code:**



**Cite this article as:** Feng S, Zhang J, Liang B, Jin H, Yuan Z. Effects of *Cyclocarya paliurus* flavonoid extract in non-alcoholic steatohepatitis mice: Intermeshing network pharmacology and *in vivo* pharmacological evaluation. Phcog Mag 2021;17:765-73.

## INTRODUCTION

Non-alcoholic steatohepatitis (NASH) is mainly characterized by hepatic lipid accumulation, inflammation, and fibrosis.[1] To date, there is no medicine to treat NASH.[2] Hence, early improvements in hepatic fat deposition play a pivotal role in the treatment of NASH.[3] *Cyclocarya paliurus* (CPF) (Batal.) Iljinsk Cyclocaryaceae, only grows in the highlands of Southern China, such as Guangdong, Guangxi, Fujian, and Yunnan, which is a unique species.[4] A number of studies have shown that *C. paliurus* flavonoid (CPF) extract has multiple bioactivities and could be beneficial in the treatment of hyperlipidemia and diabetes.[5,6] CPF can reduce fat accumulation in the liver.[7] The leaf extract of *C. paliurus* contains a variety of phytochemical components, such as polysaccharides, triterpenes, flavonoids, steroids, saponins, and phenolic compounds.[8,9] Therefore, it is important to identify the active components of CPF and their mechanism of action of inducing hepatic lipid breakdown. Similar to other natural products with multi-component, multi-target, and multi-pathway characteristics, the molecular mechanism of CPF is difficult to elucidate.

Network pharmacology can independently present the "component-target-pathway" related to specific diseases. It is a systematic and holistic approach, which conforms to the principle of holistic view and treatment based on syndrome differentiation, which can effectively promote the in-depth study of traditional Chinese medicine (TCM) compounds.[10] With the rapid development of bioinformatics, network pharmacology has become a booming field of modern research.[11,12] As the main tool of network pharmacology, network analysis based on widely available databases enables us to preliminarily understand the potential mechanism of interaction of natural products.[13,14] Pharmacological targets of online herbs were found through Traditional Chinese Medicine Systems Pharmacology Database and Analysis Platform (TCMSP), which is a unique systematic Pharmacology Platform of TCM.[15,16] Herein, we will elucidate the primary active components and signaling pathways of CPF in NASH treatment.

Peroxisome proliferator-activated receptors (PPARs) form heterodimers with retinoid X receptors. There are three subtypes of PPAR known: Peroxisome proliferator-activated receptor alpha (PPAR α), PPAR β/δ, and Peroxisome proliferator-activated receptor gamma (PPAR γ).[17] PPAR α is one of the regulatory factor for NASH, important regulatory factors affecting the metabolism of long-chain fatty acids (LCFAs) and lipoproteins controlling lipid metabolism plays an important part in the occurrence and progression of fatty liver to use.[18] (1) PPAR promotes the main mechanism of lipid metabolism: Filaments the somatic and peroxisome of the are-oxidation system and the micron–oxidation system, improve insulin resistance, promote lipid oxidation and fat content solution.[19] (2) PPAR regulates the encoding of the fatty acid transporter 1 gene to promote the absorption of fatty acids;[20] the activated PPAR can also regulate fatty acid translocation enzyme (FAT/CD 36) increasing the transport of fatty acids.[21] (3) It regulates the expression of fibroblast growth factor-21; affects the synthesis of mitochondrial 3-hydroxy-3-methyl glutaric acyl coenzyme A, carnitine palmitoyltransferase (CPT), and acyl coenzyme A oxidase 1 (ACOX1); and regulates the oxidation of fat acid molecules and the formation of ketone bodies.[22]

Therefore, in this study, we explored the potential mechanism of CPF in NASH through *in vivo* experiments and network pharmacology, so as to provide theoretical basis for further experimental research. Therefore, in this study, we aimed to evaluate the role of CPF in lipid metabolism and its molecular mechanism of action and to provide insight into mouse models of human NASH.

## MATERIALS AND METHODS

### Chemicals

The high-fat diet (HFD) was purchased from Guangdong Medical Experimental Animal Center (batch number: 20180117, formula: Sucrose, 20%; lard, 15%, cholesterol, 1.2%; sodium cholate, 0.2%; casein, 10%; calcium hydrogen phosphate, 0.6%; stone powder, 0.4%; premix, 0.4%; basal feed, 52.2%). The Bio-Rad DC™ protein assay reagent pack was purchased from Bio-Rad (Bio-Rad LaboMouseories, CA, USA). Oleic acid and palmitic acid were purchased from Sigma-Aldrich (St. Louis, MO, USA). PPAR α and PPAR γ antibodies were purchased from Cell Signaling Technology (Beverly, MA, USA). The primers were purchased from Sangon Biotech (Shanghai, China). Alanine aminotransferase (ALT), aspartate aminotransferase (AST), triglycerides (TG), total cholesterol (TC), malondialdehyde (MDA), and superoxide dismutase (SOD) assay kit were obtained from the Nanjing Jiancheng Bioengineering Institute (Nanjing Jiancheng Bioengineering Institute, Nanjing, China).

### *Cyclocarya paliurus* preparation

Leaves of *C. paliurus* were obtained from the Zhejiang Suichang Wei-Er-Kang CPF Specialty corporation. CPF was previously analyzed by high-performance liquid chromatography to identify its primary constituents.[23] The leaves were extracted twice (2 h/each) with 10 times the amount of 90% ethanol by heating (70°C) under reflux. Then, the extract was concentrated to 0.5 mg/mL, loaded onto D101 microporous adsorbent resin (5 mm × 200 mm), and eluted with distilled water until the effluents were colorless. The second eluent with 60% ethanolic solution (20 BV) was concentrated and freeze-dried (LGJ-10C freeze-drying machine, Guangzhou Shenhua Biotechnology Co., Ltd) to obtain CPF powder.

### Qualitative analysis of *Cyclocarya paliurus* and estimation of total flavonoid content

The ratio of total flavonoids in the CPF was roughly 69.21%, as detected by a Ultraviolet/Visible spectrometer and using rutin as the standard.[24] The qualitative analysis was conducted on high-performance liquid chromatography-mass spectrometry (HPLC-MS), using Thermo Scientific Accela 1250 Pump coupled with a Thermo Scientific TSQ Quantum Access MAX (Thermo Fisher, Massachusetts, USA). Chromatographic separation parameters were similar to the HPLC method of fingerprint. Later, for the *in vitro* testing, the extract was further filtered by 0.24 μm pore-size filter (Millipore, Billerica, MA, USA) and stored for <1 week at 4°C. Finally, the extract was diluted to a certain concentration with saline and phosphate-buffered saline before use.

### Animals

C57 BL/6J mice (male, 5 weeks, 16–18 g) were purchased from the Guangdong Medical LaboMouseory Animal Center (the medical experimental animal number was SCXK (YUE) 2013-0001; the animal certification number was NO. 44002100012766). Animals were housed in a temperature controlled (22°C) and humidity-controlled (70%) room with a 12 h dark–light cycle and provided with adapted feed with standard pellets. All animals used in this study were cared for humanely and in accordance with the agency's animal care guidelines, which were maintained with a treatment protocol (SYXK (Guangdong), 2020-0227) approved by Guangzhou Medical University.

## High-fat diet -induced nonalcoholic steatohepatitis model and the therapeutic effect of *Cyclocarya paliurus*

In this study, 40 male C57 BL/6J mice (16–18 g) were randomly divided into 4 groups. Each group contained 10 mice, including control (CTR), Model, Model + Metformin (MET, 100 mg/kg), and Model + CPF (250 mg/kg). The mice in the control group were fed with standard laboratory chow diet, whereas the mice in the model group were fed with HFD chow (20180117, Guangdong Medical Laboratory Animal Center). The treatment mice were orally administered with (10 mL/kg body weight, p. o.) with CPF and MET daily for up to 18 weeks, and the model and control groups were orally administered with blank solvent (0.5% CMC-Na) daily. Metformin was used as the positive control. The body and food intake weights of the mice were monitored every week.

On week 18, mice were weighed under ether anesthesia. Then, blood was collected from the abdominal aorta for biochemical evaluation. Steatohepatitis was evaluated by the levels of TG, TC, ALT, AST, MDA, and SOD using the commercial kits according to the manufacturer's instructions. The weights of the body, liver, kidney, brain, heart, spleen, testis, and abdominal fat were measured in all mice soon after sacrifice (intraperitoneal injection of 2% sodium pentobarbital solution). A portion of the liver was fixed in 4% paraformaldehyde for histological evaluation. Liver tissues were quickly frozen in liquid nitrogen for Western blot and reverse transcription polymerase chain reaction (RT-PCR) analysis. The levels of PPAR α and PPAR γ were measured using RT-PCR and Western blot.

## Network pharmacology-based analysis

First, the chemical compounds and human protein targets of these chemical compounds in CPF were retrieved in TCMSP Database.[25] Moreover, NASH-related human gene targets were found in GenBank and Drug Bank databases. The targets of CPF and NASH-related targets obtained from the first step were imported to Cytoscape software.[26] Then, Cytoscape generates a set of networks based on different biological functions, in which the different shaped nodes are represented as molecules with different functions and the biological relationship between the two nodes is represented as an edge (line). In addition, the network is ranked according to Cytoscape scores, thus representing the importance of molecules in the network. Furthermore, typical pathways are obtained in Metascape by core analysis.[27] The *P* values calculated by Fisher's exact test reflect the importance of the molecule to the typical pathway. The smaller the *P* value, the stronger the significance. Finally, Metascape was used for the comparative analysis to further study the mechanism of CPF in NASH. After the fictitious aims of the compounds within CPF and the known treatment targets of NASH were connected, the data on protein–protein interaction (PPI) were integrated and derived from the latest online String[28] database. The detailed implementation process of the network pharmacology research was shown in Supplementary Figure 1.

## RNA isolation and quantitative reverse transcription polymerase chain reaction analysis

Briefly, total RNA was extracted from tissue homogenates using Trizol reagent (Invitrogen, Carlsbad, CA, USA). Briefly, 1 μg RNA was reverse transcribed to cDNA using PrimeScript™ RT reagent Kit (TaKaRa, Kusatsu, Japan). The specific transcripts were quantified by ABI 7500 real-time PCR system (Applied Biosystems, Foster, CA, USA) using SYBR Premix Ex Taq™ II (Tli RNaseH Plus) with ROX plus (TaKaRa, Kusatsu, Japan). Primers were synthesized by Sangon Biotech and the following primer sequences were used: TGCTGCTTCTCCTATGGACG (forward) and GCTCAGTGATGTATTCTTGGACC (reverse) for PPAR α, CAGAGCTTGAGTGTGACG (forward) and TCGTACCTGATGTGCCTC (reverse) for PPAR γ, GGGATTGCTGTGGTAGTGAGC (forward) and GGTATGGAATCAACCCGTTGTC (reverse) for CYP7A1, CCAGGCACAGGAGAGTACG (forward) and GGGCAAGTGCAGCACATAG (reverse) for CYP27A1, TCTCCGGCAAGTACCAACTG (forward) and TTCCAACTGAACCACTGTCTTG (reverse) for fatty acid binding protein 1 (FABP1), ATGATGGCCAGTTCAGGAAAACAG (forward) and CAGAAACCGGATGGCAGAAAC (reverse) for CPT2 and TGGAGTCTACTGGCGTCTT (forward) and TGTCATATTTCTCGTGGTTCA (reverse) for GAPDH. The mRNA levels were normalized to GAPDH. Relative mRNA expression was calculated by the comparative $2^{-\Delta\Delta CT}$ method.

## Western blot analysis

Proteins were extracted from the cell lysate. Then, the concentration of protein was determined using a BCA kit (Biotime, Shanghai, China). Equivalent amounts of protein were electrophoresed on sodium dodecyl sulfate polyacrylamide gel (SDS-PAGE, 10% gel). The membrane was transferred onto PVDF membrane through the BIO-RAD imprinting system, sealed with 5% (W/V) skimmed milk powder, and incubated with monoclonal antibody (1:10000) at 4°C overnight. Then, the membrane was washed thrice with 0.1% Tween 20 and incubated with a horseradish peroxidase-conjugated secondary antibody (1:10,000) for 1 h. The bands were observed using an enhanced chemiluminescence system (Millipore, Billerica, MA, USA). Quantity One software (Bio-RAD, Hercules, CA, USA) was used for density analysis.

## Statistical analysis

RT-PCR and Western blot experiments were repeated at least thrice. The results are expressed as mean ± standard deviation. Data were statistically analyzed using GraphPad Prism software version 5.0 (GraphPad Software, San Diego, CA, USA). Paired *t*-test or one-way variance test was used for the statistical analysis, and $P < 0.05$ was considered statistically significant.

# RESULTS

## Effects of *Cyclocarya paliurus* on high-fat diet -induced non-alcoholic steatohepatitis mice

First, the quality of CPF was analyzed by UPLC-MS/MS, and the primary contents are as follows: isoquercitin (RT of 20.27 min, 23.98 ± 1.21 mg/g), quercetin 3-*O*-β-D-glucopyranoside (RT of 20.75 min, 6.73 ± 0.06 mg/g), quercitrin (RT of 21.12 min, 11.98 ± 0.41 mg/g), quercetin-7-rhamnoside (RT of 22.16 min, 0.96 ± 0.03 mg/g), kaempferol-3-*O*-rhamnoside (RT of 22.52 min, 18.98 ± 1.03 mg/g), quercetin (RT of 23.60 min, 2.73 ± 0.05 mg/g), luteolin (RT of 24.96 min, 0.98 ± 0.01 mg/g), and kaempferol (RT of 27.35 min, 2.84 ± 0.03 mg/g). Then, we examined the efficacy of CPF on HFD-induced NASH mice, which is widely used for testing potential therapies for NASH.[29] As loss in body weight is the major clinical feature of NASH, treatment of mice with a dosage of CPF (250 mg/kg) significantly reduced their bodyweight from day 0 to week 18 when compared with the model mice. However, Figure 1a shows that body weight of mice was further reduced after treatment with MET. Moreover, compared with the model mice, CPF-treated mice also showed decrease in the ratio of weight of organs including liver, kidney, and abdominal fat (g/g body weight), which were approached to that of normal mice [Figure 1b-d] indicating that CPF reduced multiple organ damage following inflammation. Histological studies showed that the liver tissue of mice in the control

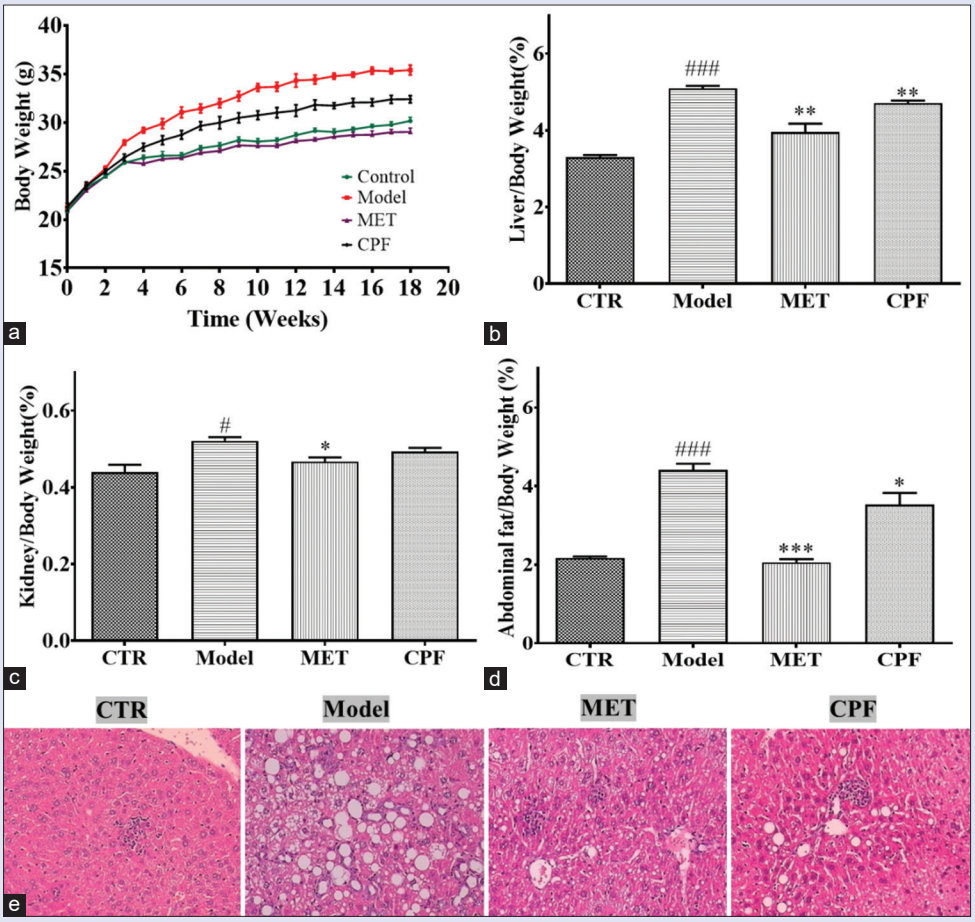


**Figure 1:** Data showing body weight. (a) Liver/body weight (b) Kidney/body weight (c) Abdominal fat/body weight (d) and liver HE staining (e) in C57BL/6 mice. Values are presented as means ± SDS ($n$ = 6). *Cyclocarya paliurus* prevented HFD-induced weight gain. Liver sections were stained with H and E. Magnification (×100). *, $P < 0.05$; **, $P < 0.01$; and ***, $P < 0.001$ compared to the model group. # $P < 0.05$; ## $P < 0.01$; and ### $P < 0.001$ compared to the control group ($n = 6$)

group was uniformly stained with regular arrangement of hepatocyte cords and clear hepatic sinuses [Figure 1e, green arrow], whereas the liver plate of mice in the model group was orderly arranged with obvious swelling of hepatocytes, mixed hepatocyte steatosis with large and small vesicles [Figure 1e, black arrow] that were filled with fat vacuoles, and hyperplasia of small bile ducts. In the CPF and MET groups, the structure of the hepatic lobules was intact, the liver plates were arranged neatly [Figure 1e, blue arrow], and the vacuoles [Figure 1e, yellow arrow] were significantly reduced.

After 18 weeks of feeding mice with HFD, typical characteristics of a fatty liver were observed in the HFD group, which included significant increase in the levels of serum TG [Figure 2a], TC [Figure 2b], ALT [Figure 2c], and AST [Figure 2d]. However, CPF decreased the levels of the aforementioned indicators. Next, we found that CPF reduced the formation of MDA [Figure 2e] and increased the activity of SOD [Figure 2f]. All these results show that CPF attenuates lipid accumulation in the hepatocytes of HFD-induced NASH mice.

## Results of network pharmacology-based analysis

All compounds of CPF were filter through TCMSP database according to oral bioavailability % ≥50% and drug likeness ≥0.1. Finally, we found 26 compounds in CPF [Supplementary Table 1] and 207 human target proteins (relevance score ≥15) of CPF [Supplementary Table 2].

Herb-Compound-Target Network was established by using Cytoscape v3.7.2. Figure 3 shows the network relationship between 26 compounds and 207 compound-related targets, which showed the interaction of targets containing 233 nodes and 579 edges. We found that 8 out of 26 compounds, such as luteolin, quercetin, kaempferol, ellagic acid, isoquercitrin, gallic acid, inositol and myricetin, regulated more than 24 identical genes. Finally, in the pharmacological study of this network, 6 (PPARA, PPARG, CYP7A1, CYP27A1, CPT2, and FABP1) out of 207 genes were simultaneously regulated by more than 8 herbal compounds. Therefore, these 8 compounds and 6 genes may be the core nodes to indicate the relationship of the herb-compound-compound target of CPF.

Supplementary Table 3 shows molecular networks constructed by NASH-related genes. Furthermore, a total of 27 targets related to NASH were screened in CPF and string was used to illustrate the interaction between these 27 targets. As shown in Figure 4b, there were 27 nodes (the average node degree was 8.29) and 126 edges. The local clustering coefficient was 0.81. In addition, $P < 0.01$ indicated that the enrichment of PPI was significant. There was a greater correlation among PPARA, PPARG, CYP7A1, CYP27A1, CPT2, and FABP1 [Figure 4a]. Therefore, these 6 genes may be the core nodes.

Based on the results of pathway enrichment of the 27 target genes, the enrichment analysis of the Kyoto Encyclopedia of genes and Genomes (KEGG) pathways was conducted. KEGG could be used

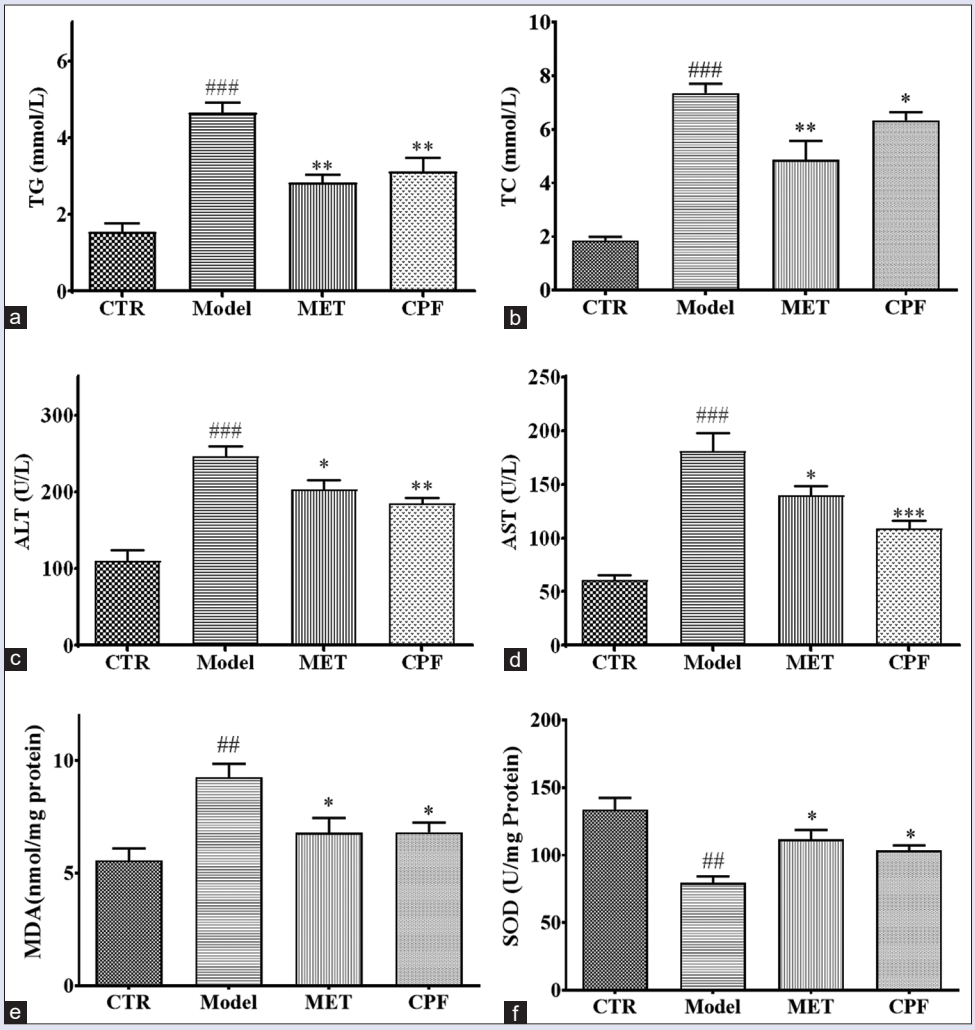


**Figure 2:** Effects of *Cyclocarya paliurus* on the liver function and oxidative stress, including triglycerides. (a), Total cholesterol (b), alanine aminotransferase (c), AST (d), malondialdehyde (e) and superoxide dismutase (f). Data are shown as mean ± SDS ($n = 6$). * $P < 0.05$; ** $P < 0.01$; and *** $P < 0.001$ compared to the model group. # $P < 0.05$; ## $P < 0.01$; and ### $P < 0.001$ compared to the control group

to predict gene enrichment pathways.[30] We found the top 10 pathways [Table 1]. The enrichment pathways were mainly concentrated in the regulation of PPAR signaling pathway, cholesterol metabolism, bile secretion, type II diabetes mellitus, activated protein kinase (AMPK) signaling pathway, insulin signaling pathway, and so on. The top 1 PPAR signaling pathway among shared signaling pathways was focused for our further research. Therefore, PPAR signaling pathway was further studied using the quantitative reverse transcription polymerase chain reaction (qRT-PCR) analysis and western blotting studies.

Table 1 Top 10 pathways enriched based on target genes (KEGG Pathway). "Count" is the number of genes in the user-provided lists with membership in the given ontology term.

## The modulation effect of *Cyclocarya paliurus* on peroxisome proliferator-activated receptor α/ peroxisome proliferator-activated receptor γ signaling pathway

To explore the mechanisms of CPF in C57BL/6 mice, we first examined the expression levels of PPAR α and PPAR γ involved in PPAR signaling pathway in mouse liver tissue. Then, molecular verification was performed with RT-PCR and Western blot analysis. The hepatic mRNA and protein expressions [Figure 5] of PPAR α and PPAR γ were significantly decreased in C57BL/6 mice when compared with the normal group ($P < 0.001$). Similarly, CPF and MET treatment significantly reversed these expression profiles toward normal. Dual PPARα/γ was upregulated by CPF in the liver of C57BL/6 mice.

Moreover, we examined the expression of CYP7A1, CYP27A1, FABP1, and CPT2, which regulate the transcription of a large number of genes involved in multiple features of lipid and lipoprotein metabolism. Interestingly, we found that the mRNA levels of FABP1, CYP7A1, and CYP27A1 were significantly increased, and the expression of CPT2 was decreased [Figure 6]. Similarly, CPF and MET treatment significantly reversed these expression profiles toward normal.

These results indicate that hepatic lipogenesis transcription factors (PPAR α and PPAR γ), as well as the uptake and hydrolysis of lipoproteins, were significantly altered in C57BL/6 mice. These changes were related to the therapeutic effects of CPF. This is consistent with the lipid droplets observed in C57BL/6 mice.

# DISCUSSION

NASH refers to the pathological changes in the liver tissue. It is similar to alcoholic hepatitis, with characteristics such as degeneration of

**Table 1:** Top 10 pathways enriched based on target genes (Kyoto Encyclopedia of genes and Genomes pathway)

| Pathway | Description | Count in gene set | False discovery rate |
|---|---|---|---|
| hsa03320 | PPAR signaling pathway | 6 of 72 | 2.14E-07 |
| hsa04979 | Cholesterol metabolism | 5 of 48 | 0.00000104 |
| hsa04976 | Bile secretion | 5 of 71 | 0.00000437 |
| hsa04930 | Type II diabetes mellitus | 4 of 46 | 0.0000341 |
| hsa04152 | AMPK signaling pathway | 5 of 120 | 0.0000341 |
| hsa04910 | Insulin signaling pathway | 5 of 134 | 0.0000447 |
| hsa05140 | Leishmaniasis | 4 of 70 | 0.0000952 |
| hsa04657 | IL-17 signaling pathway | 4 of 92 | 0.00024 |
| hsa04933 | AGE-RAGE signaling pathway in diabetic complications | 4 of 98 | 0.00027 |
| hsa05145 | Toxoplasmosis | 4 of 109 | 0.00033 |

"Count" is the number of genes in the user-provided lists with membership in the given ontology term. PPAR: Peroxisome proliferator-activated receptor; AMPK: Adenosine 5′-monophosphate-activated protein kinase; IL-17: Interleukin-17; AGE-RAGE: Advanced glycation end products-receptor for advanced glycation end products

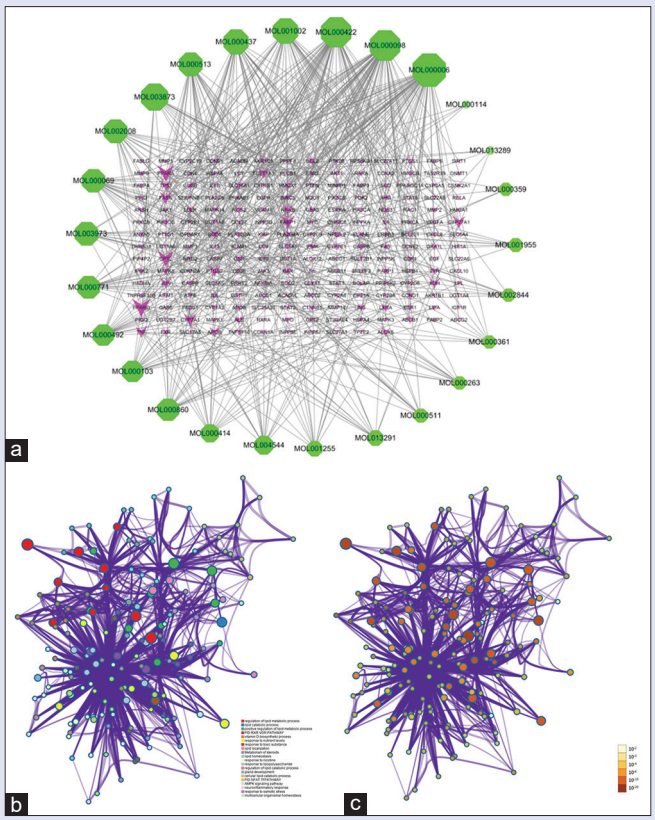


**Figure 3:** (a) Interaction network to indicate herb-compound-target composites of 26 compounds (green) and 207 targets (purple). Network of enriched terms: (b) colored by cluster ID, where nodes that share the same cluster ID are typically close to each other; (c) colored by *P* value, where terms containing more genes tend to have a more significant *P* value

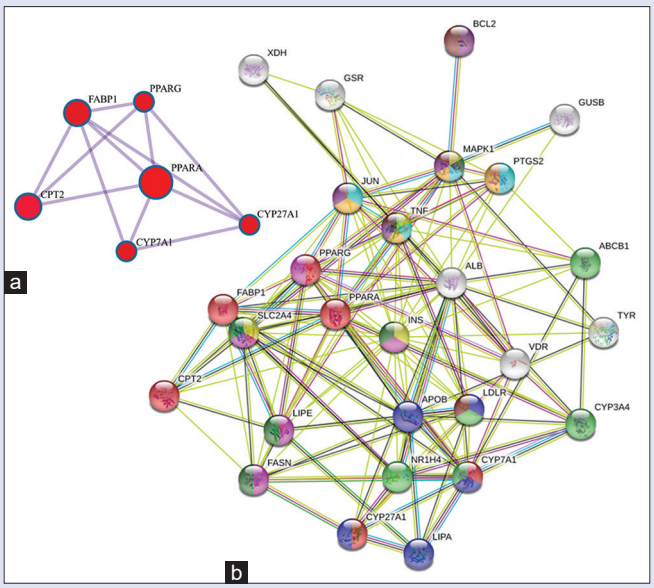


**Figure 4:** Protein-protein interaction network and MCODE components identified in the gene lists.(a)The protein–protein interaction network based on targets of *Cyclocarya paliurus* on NASH.(b) Network nodes represent different proteins. Edges represent protein-protein associations, the line thickness indicates the strength of data support. Protein–protein interaction

hepatocytes, necrosis, and inflammation. The mice NASH model is simple, inexpensive, low in animal mortality, and highly repetitive. It is a good animal model for the study of the pathogenesis of NASH and for the screening of preventive and therapeutic drugs. The body mass index, hepatic index, serum ALT, AST, TG, and TC of mice were important indexes to evaluate the model and its efficacy. In this study, we found that CPF-treated mice showed less weight gain and decrease in the levels of TG and TC. There was also a significant reduction in the levels of ALT, AST, and MDA. These results show that CPF has a good effect on mice NASH model. Therefore, we used the network pharmacological study to reveal the potential mechanism of multi-target and multi-component CPF in NASH treatment and provided scientific basis for studying its mechanism.

Network pharmacological analysis is becoming popular in studying the effect of TCM on diseases.[31] Through the network pharmacology analysis of the composition and targets of CPF, 26 compounds and 207 genes that regulated major signaling pathways, and 8 compounds and 27 genes related to NASH were finally found. There were eight key compounds detected in CPF that had an effect in treating NASH, such as luteolin, quercetin, kaempferol, ellagic acid, isoquercitrin, gallic acid, inositol, and myricetin. A total of 6 key target genes (PPAR α, PPAR γ, CPT2, FABP1, CYP7A1, and CYP27A1) related to 10 main signaling pathways (PPAR signaling pathway, cholesterol metabolism, bile secretion, type II diabetes mellitus, AMPK signaling pathway, insulin signaling pathway, and other pathways) leading to NASH were identified.

Activated PPARs can upregulate the gene expression of lipoprotein lipase[32] and promote the metabolic utilization of TG and regulation of very low-density lipoprotein. PPAR α agonists significantly improved the symptoms associated with NASH, reduced the degree of fatty liver, and delay or prevent NASH progression.[33] However, after being

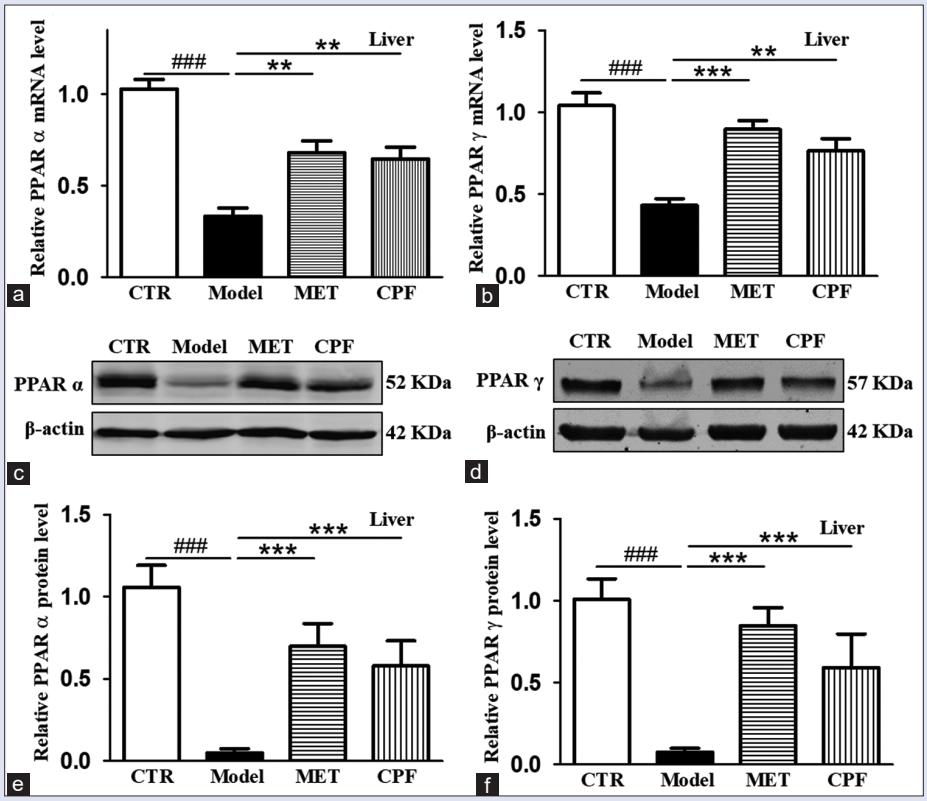


**Figure 5:** Dual peroxisome proliferator-activated receptor α/γ were upregulated by *Cyclocarya paliurus* in the liver of C57BL/6 mice. For the mRNA level of Peroxisome proliferator-activated receptor alpha (a) and Peroxisome proliferator-activated receptor gamma (b), the results were normalized to the levels of GAPDH as an internal control. The protein expression of Peroxisome proliferator-activated receptor alpha (c and e) and Peroxisome proliferator-activated receptor gamma (d and f). The level of β-actin was determined as a loading control. Values are presented as means ± SDS ($n = 6$), # $P < 0.05$, ## $P < 0.01$ ### $P < 0.001$ versus control; * $P < 0.05$, ** $P < 0.01$, *** $P < 0.01$ versus model

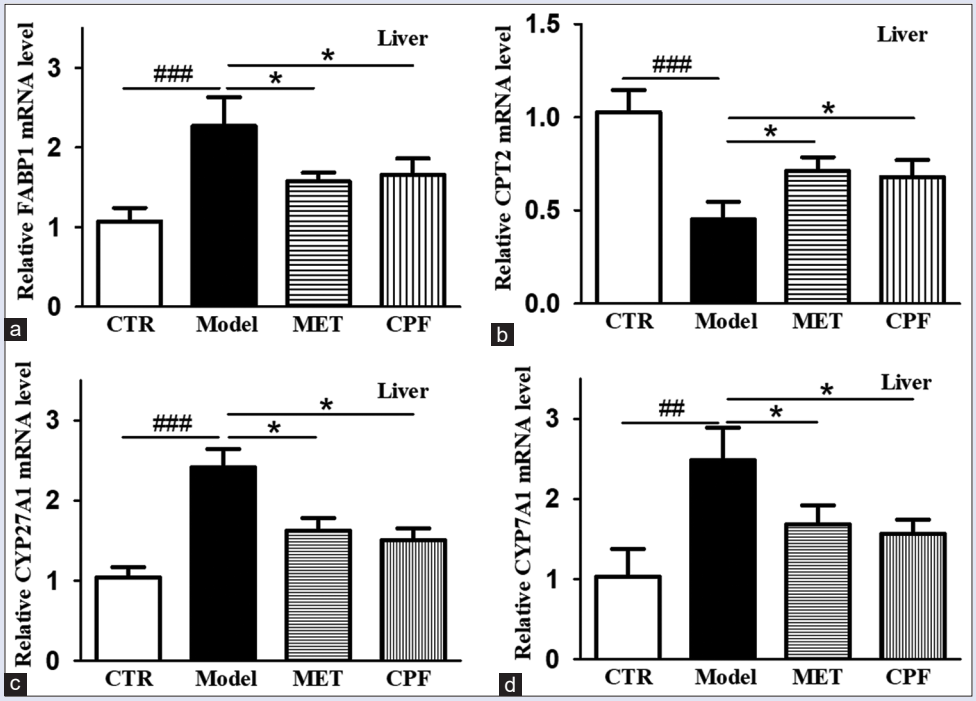


**Figure 6:** The expression of key enzymes associated with lipid metabolism in NASH mouse model. Real-time polymerase chain reaction amplification was performed for lipid metabolism genes including FABP1 (a), CPT2 (b), CYP27A1 (c), and CYP7A1 (d). Values are presented as means ± standard deviation ($n = 6$), # $P < 0.05$, ## $P < 0.01$ ### $P < 0.001$ vs. control; * $P < 0.05$, ** $P < 0.01$, *** $P < 0.01$ versus model

activated, PPAR, can increase the oxygen of fatty acids to upregulate the expression of fatty acid oxidation genes and reduce the synthesis of fatty acids and topical fatty acids, thereby reducing lipid deposition and improving insulin resistance.[34] However, can directly improve the liver lipoprotein and lipid metabolism gene, reduce liver lipid sedimentation product. Decreased activity of PPAR beam can cause disorders of energy metabolism, liver perivascular inflammation, and fat deposition, which leads to fatty liver inflammation.[35] Animal studies have shown that PPAR can induce TG formation in the liver, turbulence of lipid and carbohydrate complexes.[36] Therefore, inhibition of PPAR γ expression can cause lipoprotein anabolism disorder, fatty acid oxidation in liver decrease and liver lipid deposition, thereby accelerating the occurrence and development of fatty liver. In hepatocytes, FABP1 plays a role in lipoprotein-mediated cholesterol uptake.[37] In addition, murine FABP1 enhanced cholesterol transfer between plasma membrane and microsomes, thereby stimulating cholesterol esterification by acyl-CoA cholesterol acyltransferase *in vitro*.[36] CPT2 is associated with the oxidation disorders of the mitochondrial LCFAs. Intracellular LCFAs are esterified to acyl-CoA by the enzymes of the long-chain acyl-CoA synthase (ACSL) family and then converted to acetyl carnitine by binding with CPT1.[38] After its mitochondrial translocation via carnitine acylcarnitine translocase, acyl carnitine is converted back to acyl coenzyme A via CPT2, which then enters the fatty acid oxidation pathway (FAO), followed by the mitochondrial tricarboxylic acid cycle.[39] The CPT2 expression is mainly regulated by a transcription factor, PPAR α.[40]

Therefore, the mRNA and proteins levels were analyzed via qRT-PCR and Western blot analysis. It is noteworthy that the PPAR α/γ pathways were clearly induced in high fat + CPF mice. This suggests a positive feedback loop between the two proteins. CYP7A1 and CYP27A1, which were regulated by PPAR γ, indicating lipid metabolism, were closely associated with the pathogenesis of experimental NASH. In addition, we noticed that the expression of key lipogenic enzymes including FABP1, CYP7A1, and CYP27A1 were significantly upregulated in the liver of NASH mice, and we confirmed the significantly decreased CPT2 protein expression in HFD tissues via Western blot analysis. Moreover, after treatment of CPF, the expression of related proteins was reversed clearly, which may alleviate lipid abnormalities.

## CONCLUSION

In conclusion, CPF has been shown to be effective in reducing the hepatic accumulation of fat and shows anti-steatogenic effect by the activation of PPAR α/γ in C57BL/6J mice. As there are no approved drug therapies for NASH,[41] it is necessary to understand the mechanism of action of natural dietary products such as CPF.

### Financial support and sponsorship

This work was supported by National Natural Science Foundation of China (No. 81803689), Natural Science Foundation of Guangdong Province (No. 2018A030310292), the Third Affiliated Hospital of Guangzhou Medical University scientific research project (No. 2017B05), Foundation and Applied Basic Research Fund project of Guangdong Province (No. 2019A1515111109), Medical Research Fund project of Guangdong Province (No. A2020365) and Scientific Research Foundation of Guangdong Bureau of TCM (No. 20201213).

### Conflicts of interest

There are no conflicts of interest.

## REFERENCES

1. Lanthier N, Francque S. NASH: A welfare disease with emerging questions and adequate answer attempts. Acta Gastroenterol Belg 2020;83:339.
2. Charlton MR, Burns JM, Pedersen RA, Watt KD, Heimbach JK, Dierkhising RA. Frequency and outcomes of liver transplantation for nonalcoholic steatohepatitis in the United States. Gastroenterology 2011;141:1249-53.
3. Teramoto T, Shinohara T, Takiyama A. Computer-aided classification of hepatocellular ballooning in liver biopsies from patients with NASH using persistent homology. Comput Methods Programs Biomed 2020;195:105614.
4. Kurihara H, Asami S, Shibata H, Fukami H, Tanaka T. Hypolipemic effect of *Cyclocarya paliurus* (Batal) Iljinskaja in lipid-loaded mice. Biol Pharm Bull 2003;26:383-5.
5. Lin Z, Wu ZF, Jiang CH, Zhang QW, Ouyang S, Che CT, *et al.* The chloroform extract of *Cyclocarya paliurus* attenuates high-fat diet induced non-alcoholic hepatic steatosis in Sprague Dawley mouse. Phytomedicine 2016;23:1475-83.
6. Li J, Zhang Q, Zeng W, Wu Y, Luo M, Zhu Y, *et al.* Integrating transcriptome and experiments reveals the anti-diabetic mechanism of *Cyclocarya paliurus* formula. Mol Ther Nucleic Acids 2018;13:419-30.
7. Yao X, Lin Z, Jiang C, Gao M, Wang Q, Yao N, *et al. Cyclocarya paliurus* prevents high fat diet induced hyperlipidemia and obesity in Sprague-Dawley mouse. Can J Physiol Pharmacol 2015;93:677-86.
8. Li J, Lu Y, Su X, Li F, She Z, He X, *et al.* A no sesquiterpene lactone and a benzoic acid derivative from the leaves of *Cyclocarya paliurus* and their glucosidase and glycogen phosphorylase inhibiting activities. Planta Med 2008;74:287-9.
9. Ning ZW, Zhai LX, Huang T, Peng J, Hu D, Xiao HT, *et al.* Identification of α-glucosidase inhibitors from *Cyclocarya paliurus* tea leaves using UF-UPLC-Q/TOF-MS/MS and molecular docking. Food Funct 2019;10:1893-902.
10. Nguyen-Vo TH, Nguyen L, Do N, Nguyen TN, Trinh K, Cao H, *et al.* Plant metabolite databases: From herbal medicines to modern drug discovery. J Chem Inf Model 2020;60:1101-10.
11. Wang J, Wong YK, Liao F. What has traditional Chinese medicine delivered for modern medicine? Expert Rev Mol Med 2018;20:e4.
12. Wang YL, Cui T, Li YZ, Liao ML, Zhang HB, Hou WB, *et al.* Prediction of quality markers of traditional Chinese medicines based on network pharmacology[J].Chinese Herbal Medicines,2019,11:349-56. Available from: https://www.sciencedirect.com/science/article/pii/S1674638419300723.
13. Luo TT, Lu Y, Yan SK, Xiao X, Rong XL, Guo J. Network pharmacology in research of Chinese medicine formula: Methodology, application and prospective. Chin J Integr Med 2020;26:72-80.
14. Chen L, Huang X, Wang H, Shao J, Luo Y, Zhao K, *et al.* Integrated metabolomics and network pharmacology strategy for ascertaining the quality marker of flavonoids for Sophora flavescens. J Pharm Biomed Anal 2020;186:113297.
15. Huang T, Ning Z, Hu D, Zhang M, Zhao L, Lin C, *et al.* Uncovering the mechanisms of chinese herbal medicine (MaZiRenWan) for functional constipation by focused network pharmacology approach. Front Pharmacol 2018;9:270.
16. Zhao M, Chen Y, Wang C, Xiao W, Chen S, Zhang S, *et al.* Systems pharmacology dissection of multiscale mechanisms of action of Huo-Xiang-Zheng-Qi formula for the treatment of gastrointestinal diseases. Front Pharmacol 2019;9:1448.
17. Khatol P, Saraf S, Jain A. Peroxisome proliferated activated receptors (PPARs): Opportunities and challenges for ocular therapy. Crit Rev Ther Drug Carrier Syst 2018;35:65-97.
18. Jain MR, Giri SR, Bhoi B, Trivedi C, Rath A, Rathod R, *et al.* Dual PPAR α/γ agonist saroglitazar improves liver histopathology and biochemistry in experimental NASH models. Liver Int 2018;38:1084-94.
19. Xin GZ, Zhao ZH, Zhang RN, Pan Q, Gong ZZ, Sun C, *et al.* Folic acid attenuates high-fat diet-induced steatohepatitis via deacetylase SIRT1-dependent restoration of PPARα[J].World Journal of Gastroenterology,2020,26:2203-20. Available from: https://pubmed.ncbi.nlm.nih.gov/32476787/
20. Mu PY, Chu CC, Yu D, Shao Y, Zhao SZ. PPARγ: The dominant regulator among PPARs in dry eye lacrimal gland and diabetic lacrimal gland. Int J Ophthalmol 2020;13:860-9.
21. Zhu JZ, Yi HW, Huang W, Pang T, Zhou HP, Wu XD. Fatty liver diseases, mechanisms, and potential therapeutic plant medicines. Chin J Nat Med 2020;18:161-8.
22. Vluggens O, Andreoletti P, Viswakarma N, Jia Y, Matsumoto K, Kulik W, *et al.* Functional significance of the two ACOX1 isoforms and their crosstalks with PPARα and RXRα. Lab Invest 2010;90:696-708. Available from: https://www.nature.com/articles/labinvest201046/.
23. Zhongwen Y, Huahua X, Liuting Z. Effects of *Cyclocarya paliurus* flavonoids on insulin

resistance in obesity rat. Pharm Clin Chin Herb Med 2019;35:50-5.

24. Lin A, Li J, Li D, Jin H, Liu Y. Tissue distribution study of mangiferin after intragastric administration of mangiferin monomer, rhizoma anemarrhenae, and rhizoma anemarrhenae-phellodendron decoctions in normal or type 2 diabetic rats by LC-MS/MS. J Chromatogr B Analyt Technol Biomed Life Sci 2019;1122-1123:18-22.
25. Ru J, Li P, Wang J, Zhou W, Li B, Huang C, *et al.* TCMSP: A database of systems pharmacology for drug discovery from herbal medicines. J Cheminform 2014;6:13.
26. Bauer-Mehren A. Integration of genomic information with biological networks using Cytoscape. Methods Mol Biol 2013;1021:37-61.
27. Zhou Y, Zhou B, Pache L, Chang M, Khodabakhshi AH, Tanaseichuk O, *et al.* Metascape provides a biologist-oriented resource for the analysis of systems-level datasets. Nat Commun 2019;10:1523.
28. Szklarczyk D, Gable AL, Lyon D, Junge A, Wyder S, Huerta-Cepas J, *et al.* STRING v11: Protein-protein association networks with increased coverage, supporting functional discovery in genome-wide experimental datasets. Nucleic Acids Res 2019;47:D607-13.
29. Kučera O, Garnol T, Lotková H, Staňková P, Mazurová Y, Hroch M, *et al.* The effect of rat strain, diet composition and feeding period on the development of a nutritional model of non-alcoholic fatty liver disease in rats. Physiol Res 2011;60:317-28.
30. Di S, Han L, Wang Q, Liu X, Yang Y, Li F, *et al.* A network pharmacology approach to uncover the mechanisms of shen-Qi-Di-huang decoction against diabetic nephropathy. Evid Based Complement Alternat Med 2018;2018:7043402.
31. Wang Y, Hu B, Feng S, Wang J, Zhang F. Target recognition and network pharmacology for revealing anti-diabetes mechanisms of natural product. J Comput SCI Neth 2020;45:101186. Available from: https://www.sciencedirect.com/science/article/abs/pii/S1877750320304877.
32. Kallwitz ER, McLachlan A, Cotler SJ. Role of peroxisome proliferators-activated receptors in the pathogenesis and treatment of nonalcoholic fatty liver disease. World J Gastroenterol 2008;14:22-8.
33. Li Z, Xu Y, Cai Z, Wang X, Ren Q, Zhou Z, *et al.* Discovery of novel dual PPARα/δ agonists based on benzimidazole scaffold for the treatment of non-alcoholic fatty liver disease. Bioorg Chem 2020;99:103803.
34. Jun T, Shuilan Z, Bingtao L, Xu G, Luo X, Jiang L, *et al.* Gegen qinlian decoction coordinately regulates PPARγ and PPARα to improve glucose and lipid homeostasis in diabetic rats and insulin resistance 3T3-L1 adipocytes. Front Pharmacol 2020;11:811.
35. Zhang Q, Kong X, Yuan H, Guan H, Li Y, Niu Y. Mangiferin improved palmitate-induced-insulin resistance by promoting free fatty acid metabolism in HepG2 and C2C12 cells via PPARα: Mangiferin improved insulin resistance. J Diabetes Res 2019;2019:2052675. Available from: https://pubmed.ncbi.nlm.nih.gov/30809553/
36. Guo Q, Li F, Duan Y, Wen C, Wang W, Zhang L, *et al.* Oxidative stress, nutritional antioxidants and beyond. Sci China Life Sci 2020;63:866-74.
37. Huang H, McIntosh AL, Landrock KK, Landrock D, Storey SM, Martin GG, *et al.* Human FABP1 T94A variant enhances cholesterol uptake. Biochim Biophys Acta 2015;1851:946-55.
38. Fujiwara N, Nakagawa H, Enooku K, Kudo Y, Hayata Y, Nakatsuka T, *et al.* CPT2 downregulation adapts HCC to lipid-rich environment and promotes carcinogenesis via acylcarnitine accumulation in obesity. Gut 2018;67:1493-504.
39. Schooneman MG, Vaz FM, Houten SM, Soeters MR. Acylcarnitines: Reflecting or inflicting insulin resistance? Diabetes 2013;62:1-8.
40. Hashimoto T, Cook WS, Qi C, Yeldandi AV, Reddy JK, Rao MS. Defect in peroxisome proliferator-activated receptor alphainducible fatty acid oxidation determines the severity of hepatic steatosis in response to fasting. J Biol Chem 2000;275:28918-28.
41. Lomonaco R, Sunny NE, Bril F, Cusi K. Nonalcoholic fatty liver disease: Current issues and novel treatment approaches. Drugs 2013;73:1-14.